Round-Robin Burst Assembly and Constant Transmission Scheduling for Optical Burst Switching Networks

Takuji Tachibana, Tomoya Ajima, and Shoji Kasahara

Abstract

In this paper, we propose a round-robin burst assembly and constant burst transmission for optical burst switching (OBS) network. In the proposed method, ingress edge node has multiple buffers where IP packets are stored depending on their egress edge nodes, and bursts are assembled at the buffers in round-robin manner. Moreover, bursts are transmitted at fixed intervals with scheduler. To evaluate the performance of the proposed method, we construct a loss model with deterministic and Poisson arrivals, and explicitly derive burst loss probability, burst throughput, and data throughput. In numerical examples, we show the effectiveness of our analysis and compare the performance of the proposed method with Erlang loss system.

Index Terms: Optical burst switching, Round-robin burst assembly, Constant transmission scheduling, Queueing analysis

I. Introduction

Optical burst switching (OBS) has received considerable attention as one of the most promising technologies for supporting the next-generation Internet in wavelength division multiplexing (WDM) network [1], [3], [12], [13], [14]. In OBS network, multiple IP packets are assembled into a burst with variable length at an edge node and is transmitted from ingress node to egress one. A burst is pure payload and has a related control packet which contains control information such as burst length and routing information [4].

In order to reduce signaling delay, source node starts burst transmission without receiving any acknowledgement from egress edge node. As for the signaling protocol, just-in-time (JIT) and just-enough-time (JET) have been proposed [4], [7], [8]. In JIT, a wavelength for burst transmission is reserved using two control packets: setup and release packets [11]. A source node first sends a setup packet to reserve a wavelength and after some offset time, the associated burst is transmitted without waiting for acknowledgment. Then the source node sends a release packet to release the wavelength.

Similarly, in JET, a source node sends a control packet and then sends a burst after some offset time. The different feature from JIT is that wavelength is reserved during the burst duration indicated in the control packet [6], [13], [14]. Therefore the overhead of control packet decreases and wavelength is utilized efficiently. The readers are referred to [2] for details.

Burst assembly is also an important issue in OBS and several burst assembly techniques have been proposed. Most techniques are classified into threshold-based and timer-based burst assemblies. [9]

T. Tachibana is with the Graduate School of Information Science, Nara Institute of Science and Technology, Takayama 8916-5, Ikoma, Nara 630-0192, Japan (email:takuji-t@is.aist-nara.ac.jp).

T. Ajima is with Fourth Patent Examination Department, Japan Patent Office, Kasumigaseki 3–4–3, Chiyoda–ku, Tokyo 100–8915, Japan.

S. Kasahara is with the Graduate School of Information Science, Nara Institute of Science and Technology, Takayama 8916-5, Ikoma, Nara 630-0192, Japan (email:kasahara@is.aist-nara.ac.jp).

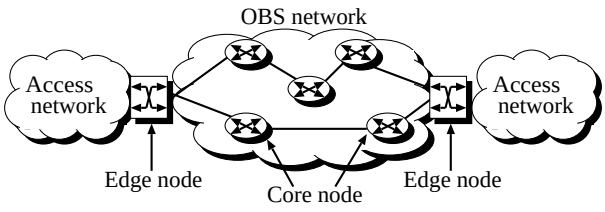

Fig. 1. OBS network.

and [10] have proposed a threshold-based burst assembly technique which utilizes a threshold as a parameter to determine the number of packets in a burst to be assembled.

In [3], timer-based burst assembly technique has been proposed. In this technique, a time counter is started at the arrival time of first packet and a burst is assembled when the time counter reaches a pre-specified value. [2] has proposed the extended timer-based technique called assured horizon which has introduced a coarse-grained bandwidth reservation.

The assembled burst is sent into OBS network after some offset time calculated according to burst scheduling. In [10], first-come first served (FCFS), priority queueing (PQ), weighted round-robin (WRR), and waiting time priority (WTP) have been considered. Among their scheduling principles, [10] has adopted FCFS where bursts are served in the same order that they are assembled.

Most of burst assembly and scheduling techniques, however, are rather complex and have difficulty in implementation. In this paper, we propose round-robin burst assembly and constant burst transmission for OBS network. In our proposed method, a burst is assembled in round-robin manner and assembled bursts are transmitted into OBS network at fixed intervals. The strong point of round-robin discipline is that timer-based burst assembly is easily implemented. We evaluate the performance of the proposed method at edge node using a loss model with deterministic and Poisson arrivals and derive performance measures explicitly.

The rest of the paper is organized as follows. Section II describes the round-robin burst assembly, and in Section III, we represent our analytical model. In section IV, we explain the performance analysis of the proposed method and numerical examples are shown in Section V. Finally, conclusions are presented in Section VI.

II. Round-robin burst assembly

The OBS network consists of edge and core nodes as shown in Fig. 1. In the OBS network, data is transmitted with burst consisting of multiple IP packets. Burst is assembled at ingress edge node and is transmitted to egress edge node. At core node, burst is switched in optical domain.

Round-robin burst assembly is performed at ingress edge node which consists of a burstifier, a scheduler, and an OBS switch (see Fig. 2). The burstifier has multiple buffers and IP packets arriving from access network are stored in the buffers depending on their egress edge nodes. Bursts are assembled with multiple IP packets stored in each buffer and burst assembly at each buffer is processed in round-robin fashion. Burst assembly processing time at each buffer is constant and we define the cycle time of round-robin as the total processing time at all buffers. Therefore, in each buffer, bursts are assembled with IP packets stored during the cycle time.

The scheduler sends the associated control packet to the egress edge node before transmitting the burst and it transmits the burst into the OBS network after some offset time. In our proposed method, the scheduler sends control packets so that bursts depart from the scheduler at fixed intervals. That is, bursts are transmitted to the burst switch at fixed intervals.

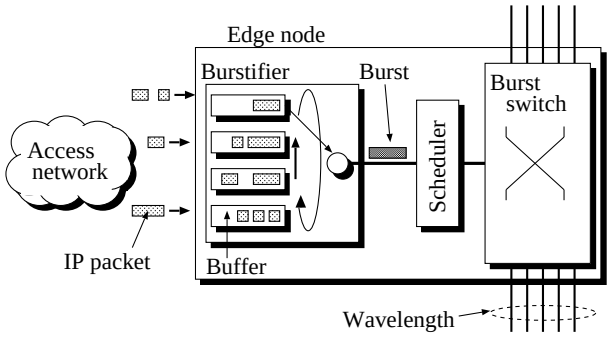

Fig. 2. Round-robin burst assembly.

In the burst switch, wavelengths are used not only by bursts from the scheduler but also by those from other OBS nodes. When there are no available output wavelengths, control packets cannot reserve wavelengths, and hence bursts cannot be transmitted to its egress edge node and those are lost.

III. Analytical model

We focus on an ingress edge node where bursts are assembled in round-robin fashion. In the burstifier of the edge node, there are L buffers as shown in Fig. 3 and IP packets coming from access network are stored in the buffers.

We assume that IP packets arrive at the edge node from the access network according to a Poisson process with rate λ and that egress edge nodes of IP packets are equally likely. Because each IP packet is stored in a buffer depending on its egress node, IP packets arrive at each buffer according to a Poisson process with rate λ/L. Moreover, we assume that the mean length of an arriving IP packet is M bits. When the transmission speed of a wavelength is B bps, an IP packet is transmitted with the mean transmission time equal to $1/\mu = M/B$.

The processing time of a burst assembly at a buffer is a fixed time equal to T. A burst is assembled with multiple IP packets which are stored during the cycle time LT. Hence the mean transmission time of a burst is given by $\lambda T/\mu = \lambda MT/B$.

The assembled bursts are forwarded to the scheduler. Then the bursts depart from the scheduler at fixed intervals equal to T and are transmitted to egress edge nodes with W output wavelengths. We assume that the bursts transmitted from other nodes arrive at the output wavelengths according to a Poisson process with rate λ_o and that the mean transmission time of the bursts is also given by $\lambda T/\mu$.

From the above assumptions, we have a D,M/M/W/W queueing model and in the following, we

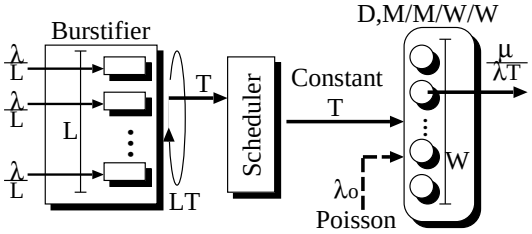

Fig. 3. Analytical model.

analyze the performance of the round-robin burst assembly with the model.

IV. Performance analysis

In this section, we explicitly derive burst loss probability, burst throughput, and data throughput with our analytical model as shown in Fig. 3. In the following, we assume that the system is in equilibrium.

Let $N(t)$ denote the number of bursts being transmitted in the system at time t. Here we assume that the first burst arrival from scheduler occurs at time 0 and we have $N(0) = 1$. First, we focus on the arrival of burst which departs from scheduler, and consider the state of system at its arrival point.

We define the number of bursts in the system just before the nth arrival of burst from scheduler as $N_n^- = N(nT^-)$ $(n = 0, 1, \cdots,)$. With the assumptions of Poisson arrival and exponential service for bursts transmitted from other nodes, the process $\{N_n^- : n = 0, 1, \cdots\}$ is a discrete-time Markov chain. We define the steady state probability for the Markov chain as

$$q_k = \lim_{n\to\infty} P_r\{N_n^- = k\}, \;\; 0 \le k \le W. \tag{1}$$

To derive the transition probability of q_k, we focus on the state transition between N_n^- and N_{n+1}^-. It is easily seen that the state transition between N_n^- and N_{n+1}^- is the same as an M/M/W/W queueing model in which the arrival process is Poisson with rate λ_o and the service time is exponentially distributed with the mean $\lambda T/\mu$. The state transition diagram for the M/M/W/W queueing model is illustrated in Fig. 4. Let $\boldsymbol{Q}$ denote the infinitesimal generator of the M/M/W/W. Note that $\boldsymbol{Q}$ is a $(W+1)\times(W+1)$ matrix whose (i,j)th element is given by

$$[\boldsymbol{Q}]_{ij} = \begin{cases} \lambda_o, & 1 \le i \le W, \;\; j = i+1, \\ -\left\{\lambda_o + \frac{(i-1)\mu}{\lambda T}\right\}, & 1 \le i \le W+1, \;\; j = i, \\ \frac{(i-1)\mu}{\lambda T}, & 2 \le i \le W+1, \;\; j = i-1, \\ 0, & \text{otherwise.} \end{cases} \tag{2}$$

For s and t $(0 \le s < t < T)$, we define $\boldsymbol{H}(s,t)$ as the state transition probability matrix from the state at time s to the state at time t, and $\boldsymbol{H}(s,t)$ satisfies the forward Chapman-Kolmogorov equation

$$\frac{\partial \boldsymbol{H}(s,t)}{\partial t} = \boldsymbol{H}(s,t)\boldsymbol{Q}. \tag{3}$$

In the following, $\boldsymbol{H}(0,t) \equiv \boldsymbol{H}(t)$ and $\boldsymbol{I}$ is the identity matrix. With the initial condition $\boldsymbol{H}(0) = \boldsymbol{I}$ and (3), $\boldsymbol{H}(t)$ is given by $\boldsymbol{H}(t) = e^{\boldsymbol{Q}t}$.

Note that the time interval between the nth and the $n+1$st observation points is T and that the system state at nth arrival point is $\min(N_n^- + 1, W)$. The transition probabilities for q_k are then given by

$$\begin{aligned} U_{ij} &\equiv P_r\{N_{n+1}^- = j | N_n^- = i\}, \\ &= \begin{cases} [\boldsymbol{H}(T)]_{i+1,j}, & 0 \le i \le W-1, \;\; 0 \le j \le W, \\ [\boldsymbol{H}(T)]_{W,j}, & i = W, \;\; 0 \le j \le W. \end{cases} \end{aligned} \tag{4}$$

With $\boldsymbol{U} = [U_{ij}]$, $\boldsymbol{q} = (q_0, \cdots, q_W)$, and $\boldsymbol{e} = (1, \cdots, 1)^T$, $\boldsymbol{q}$ is determined from the equilibrium equations $\boldsymbol{q} = \boldsymbol{q}\boldsymbol{U}$ and the normalizing condition $\boldsymbol{q}\boldsymbol{e} = 1$. Hence the loss probability of burst which departs from the scheduler is given by q_W.

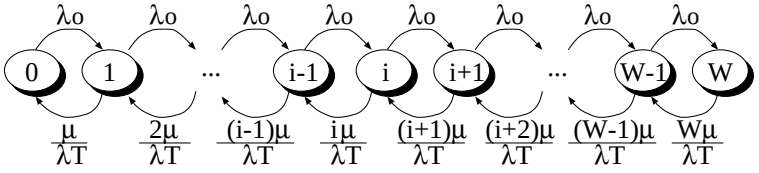

Fig. 4. State transition diagram.

Next, we consider the steady-state probability at an arbitrary point defined as $p_k = \lim_{t\to\infty} P_r\{N(t) = k\}$. We define the nth cycle as the time interval $[nT, (n+1)T)$. From the assumptions in our analytical model, it is clear that the process $N(t)$ regenerates itself at nT $(n = 0, 1, \cdots)$. With the renewal-reward theorem [15, p. 60], we have for $k = 0, 1, 2, \cdots$,

$$p_k = \lim_{t\to\infty} \frac{1}{t}\int_0^t \mathbf{1}_{\{N(t)=k\}} dt = \frac{1}{T}\int_0^{T^-} E\left[\mathbf{1}_{\{N(t)=k\}}\right] dt, \tag{5}$$

where $\mathbf{1}_{\{X\}}$ is the indicator function of event X. In the following, we consider time average of the number of bursts in the system over one cycle.

Let $\{r_k : k = 0, \cdots, W\}$ denote the state probability at the beginning of a cycle. With the steady state probability q_k, r_k is given by the following equations.

$$r_k = \begin{cases} 0, & k = 0, \\ q_{k-1}, & 0 < k < W, \\ q_{W-1} + q_W, & k = W. \end{cases} \tag{6}$$

Let $\boldsymbol{p} = (p_0, \cdots, p_W)$ and $\boldsymbol{r} = (r_0, \cdots, r_W)$. For $0 \le t < T$, we have

$$E\left[\mathbf{1}_{\{N(t)=k\}}\right] = \left[\boldsymbol{r}e^{\boldsymbol{Q}t}\right]_k, \tag{7}$$

where $[\boldsymbol{x}]_k$ denote the kth element of vector $\boldsymbol{x}$. Substituting (7) into (5), we obtain

$$\boldsymbol{p} = \frac{1}{T}\boldsymbol{r}\int_0^{T^-} e^{\boldsymbol{Q}t} dt = \frac{1}{T}\boldsymbol{r}\sum_{k=0}^{\infty} \frac{\boldsymbol{Q}^k T^{k+1}}{(k+1)!}, \tag{8}$$

where we use the continuity of $e^{\boldsymbol{Q}t}$ in the last equality.

In (8), $\boldsymbol{Q}$ is the infinitesimal generator of M/M/W/W and hence $\boldsymbol{Q}$ is singular. Now we consider the matrix $\boldsymbol{e\pi} - \boldsymbol{Q}$ where $\boldsymbol{\pi}$ is the steady-state probability vector of M/M/W/W such that $\boldsymbol{\pi Q} = \boldsymbol{0}$ and $\boldsymbol{\pi e} = 1$. Noting that $\boldsymbol{e\pi} - \boldsymbol{Q}$ is nonsingular [5], we have

$$\boldsymbol{Q} = \boldsymbol{Q}^2(\boldsymbol{Q} - \boldsymbol{e\pi})^{-1}. \tag{9}$$

With (8) and (9), $\boldsymbol{p}$ is explicitly given by

$$\boldsymbol{p} = \frac{1}{T}\boldsymbol{r}\left\{\boldsymbol{I}T + (e^{\boldsymbol{Q}T} - \boldsymbol{I} - \boldsymbol{Q}T)(\boldsymbol{Q} - \boldsymbol{e\pi})^{-1}\right\}. \tag{10}$$

Because Poisson arrivals see time average (PASTA) [15], the loss probability for the bursts from other nodes is given by p_W.

With q_W and p_W, the burst loss probability P_{loss} is given by the following equation.

$$P_{loss} = \frac{q_W + \lambda_o T p_W}{1 + \lambda_o T}. \tag{11}$$

The burst throughput defined as the number of transmitted bursts per unit of time, $T_{hr}^{(b)}$, is given by

$$T_{hr}^{(b)} = \frac{1 - q_W}{T} + \lambda_o (1 - p_W). \tag{12}$$

Finally, the data throughput defined as the amount of transmitted data (bits) per unit of time, $T_{hr}^{(d)}$, is derived as

$$T_{hr}^{(d)} = \lambda M \left\{ (1 - q_W) + \lambda_o T (1 - p_W) \right\}. \tag{13}$$

V. Numerical examples

In the following, we assume that the transmission speed of each output wavelength is $B = 10$ Gbps. Moreover, we assume that IP packets with the mean size of 1250 bytes, i.e. $M = 10,000$, arrive at edge node from access network. Thus, the mean transmission speed of an IP packet, $1/\mu$, is 1.0 μs and the unit of time is 1.0 μs in the following. In this section, we set $L = 5$ and $\mu = 1.0$.

A. Impact of burst assembly processing time

First, we consider how burst assembly processing time T affects burst loss probability, burst throughput, and data throughput. Here, we set $W = 32$ and $\lambda = 1.0$. λ_o is determined so that the system utilization factor $\rho = \lambda(1 + \lambda_o T)/W\mu$ is constant.

Fig. 5 illustrates the loss probability against burst assembly processing time with $\rho = 0.5$, 0.75, 1.0, and Fig. 6 illustrates the burst and data throughputs. These results are calculated by our analysis and simulation. From both figures, we observe that analytical and simulation results are almost the same regardless of T and ρ.

Fig. 5 shows that the burst loss probability does not change as the burst assembly processing time becomes large. When the burst assembly processing time is large, large bursts are assembled at

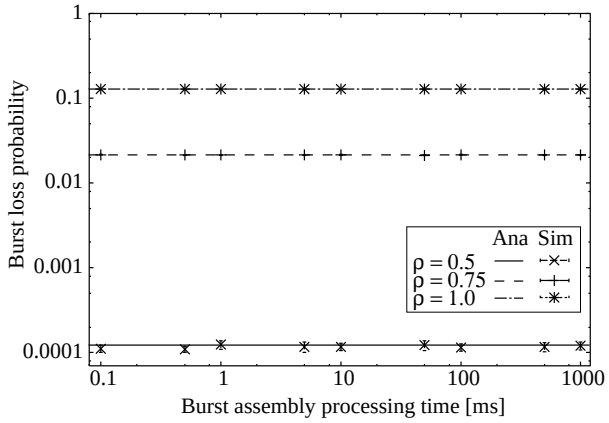

Fig. 5. Burst loss probability vs. burst assembly processing time.

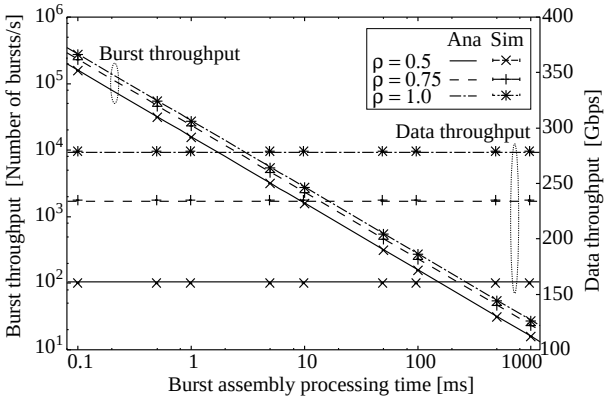

Fig. 6. Burst and data throughputs vs. burst assembly processing time.

edge node. However, burst transmission interval also becomes large. Therefore the burst assembly processing time does not affect the burst loss probability in our proposed method. In Fig. 5, we also find that the burst loss probability becomes large as the system utilization factor ρ increases.

From Fig. 6, we observe that the burst throughput becomes small as the burst assembly processing time increases. This is because the increase of burst assembly processing time causes large burst transmission interval. As a result, the transmission delay of burst becomes large and the number of transmitted bursts per unit of time becomes small. The burst throughput also decreases as the system utilization factor becomes small, however, the impact of the system utilization factor on the burst throughput is smaller than that of the burst assembly processing time. On the other hand, the data throughput does not change as the burst assembly processing time becomes large.

From these observations, the burst loss probability and data throughput do not change as burst assembly processing time becomes large. However, the transmission delay of burst becomes large and the burst throughput decreases.

B. Impact of bursts transmitted from other nodes

Next we investigate how bursts transmitted from other nodes affect the performance of round-robin burst assembly. We also consider another burst scheduling in which bursts are transmitted at exponential intervals. This burst scheduling corresponds to the well-known Erlang loss system. The loss probability, burst throughput, and data throughput in the case of exponential intervals are given by Erlang loss formula.

Fig. 7 shows the relation between arrival rate of bursts transmitted from other nodes, λ_o, and burst loss probability in the cases of $\lambda = 3.0$, 5.0, and 10.0. Fig. 8 shows the results for burst and data throughputs. Here, we set $W = 32$ and $T = 1.0$ ms. In both figures, the analytical results are almost the same as the simulation results regardless of λ_o and λ.

From Fig. 7, we observe that the burst loss probability for the round-robin burst assembly increases as the arrival rate of bursts transmitted from other nodes becomes large. This is simply because the system is overloaded. We also observe that the burst loss probability increases as the arrival rate of packets from access network becomes large. This is because large bursts are assembled with many IP packets at each edge node.

Comparing the loss probabilities for fixed and exponential interval cases in Fig. 7, we can see that the loss probability for the fixed interval case is smaller than or equal to one for the exponential one

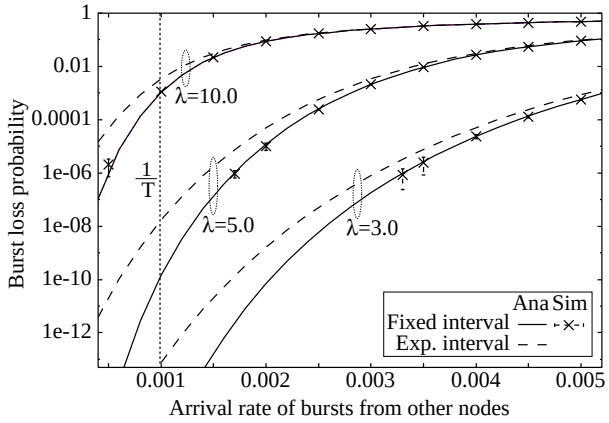

Fig. 7. Burst loss probability vs. arrival rate of bursts from other nodes.

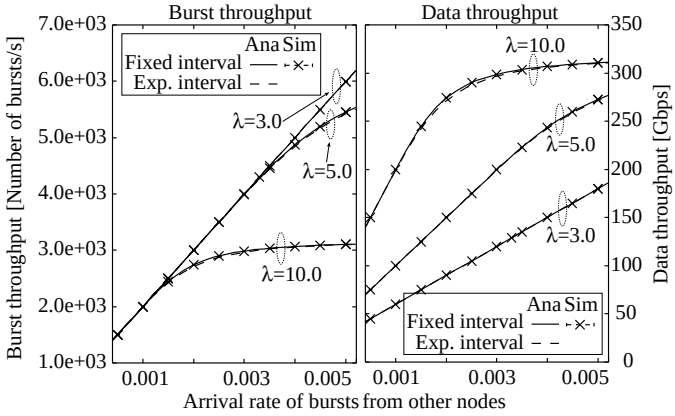

Fig. 8. Burst and data throughputs vs. arrival rate of bursts from other nodes.

when λ_o is greater than 0.001. This implies that the scheduler with the fixed interval transmission is effective when the arrival rate of burst transmitted from other nodes is larger than the arrival rate of burst from the scheduler. Moreover, the loss probability for the fixed interval case decreases as λ becomes small. Therefore, the scheduler with the fixed interval transmission is effective when the traffic load is small.

From Fig. 8, we observe that the burst and data throughputs become large and converge to constant values as the arrival rate of bursts transmitted from other nodes increases. We find that the burst throughput becomes small as the arrival rate of IP packets from access network, λ, increases. This is because the length of burst becomes large and this results in the increase of the burst loss probability. However, the number of packets assembled into a burst also increase and this causes large data throughput.

C. Impact of the number of wavelengths

Fig. 9 shows how the number of wavelengths affects loss probabilities for the two burst scheduling with fixed and exponential intervals. In this figure, we set $\lambda = 10.0$ and $T = 1.0$ ms. The loss probabilities are calculated by analysis and simulation in the cases of $\lambda_o = 0.001$, 0.002, 0.003

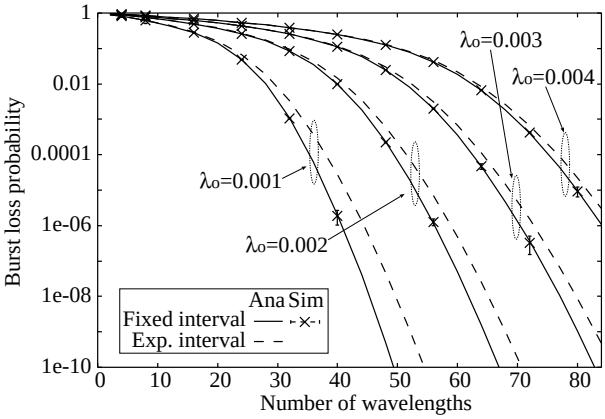

Fig. 9. Burst loss probability vs. number of wavelengths.

and 0.004. From this figure, we also find that the analytical results are almost the same as the simulation results regardless of W and λ_o. Hence our analysis is efficient to evaluate the performance of round-robin burst assembly.

From Fig. 9, we observe that the loss probability for the fixed interval case is smaller than or equal to one for that in the exponential interval case. We find that the difference between the both loss probabilities becomes large as the number of wavelengths increases. Therefore round-robin burst assembly is effective in OBS network where many wavelengths are multiplexed into an optical fiber and many fibers are used.

VI. Conclusions

In this paper, we proposed a round-robin burst assembly in which bursts are assembled at edge node in round-robin manner and are transmitted to egress edge node at fixed intervals with scheduler. To evaluate the performance of the proposed method, we considered the loss model with deterministic and Poisson arrivals and explicitly derived burst loss probability, burst throughput, and data throughput. In numerical examples, we observed that our analysis is efficient to evaluate the performance of our proposed method. Comparing the results of Erlang loss system, the round-robin burst assembly is effective for OBS network where a number of wavelengths are utilized and the arrival rate of bursts transmitted from other nodes is relatively small. Therefore a round-robin burst assembly is effective for OBS networks with mesh topology.

References

[1] A. Detti and M. Listanti, "Impact of Segments Aggregation on TCP Reno Flows in Optical Burst Switching Networks," in *Proc. IEEE INFOCOM 2002*, June 2002.

[2] K. Dolzer, "Assured Horizon - A New Combined Framework for Burst Assembly and Reservation in Optical Burst Switched Networks," in *Proc. NOC 2002*, June 2002.

[3] A. Ge and F. Callegati, "On Optical Burst Switching and Self-Similar Traffic," *IEEE Commun. Lett.*, vol. 4, no. 3, pp. 98-100, Mar. 2000.

[4] C. F. Hsu, T. L. Liu, and N. F. Huang, "Performance Analysis of Deflection Routing in Optical Burst-Switched Networks," in *Proc. IEEE INFOCOM 2002*, June 2002.

[5] D. Lucantoni, K. S. Meier-Hellstern, and M. F. Neuts, "A Single Server Queue with Server Vacations and a Class of Non-renewal Arrival Processes," *Adv. Appl. Probab.,* vol. 22, pp. 676-705, 1990.

[6] C. Qiao and M. Yoo, "Optical Burst Switching (OBS) - A New Paradigm for an Optical Internet," *J. High Speed Network*, vol. 8, no. 1, pp. 69-84, Jan. 1999.

[7] C. Qiao and M. Yoo, "Choices, Features and Issues in Optical Burst Switching," *Optical Net. Mag.*, vol. 1, no. 2, pp. 36-44, Apr. 2000.

[8] C. Qiao, "Labeled Optical Burst Switching for IP-over-WDM Integration," *IEEE Commun. Mag.*, vol. 38, no. 9, pp. 104-114, Sept. 2000.

[9] V. M. Vokkarane, K. Haridoss, and J. P. Jue, "Threshold-based Burst Assembly Policies for QoS Support in Optical Burst-Switched Networks," in *Proc. SPIE OptiComm 2002*, July 2002, pp. 125-136.

[10] V. M. Vokkarane, Q. Zhang, J. P. Jue, and B. Chen, "Generalized Burst Assembly and Scheduling Techniques for QoS Support in Optical Burst-Switched Networks," in *Proc. IEEE Globecom 2002*, Nov. 2002.

[11] J. Y. Wei and R. I. McFarland, "Just-In-Time Signaling for WDM Optical Burst Switching Networks," *J. Lightwave Tech.*, vol. 18, no. 12, pp. 2019-2037, Dec. 2000.

[12] J. White, M. Zukerman, and H. L. Vu, "A Framework for Optical Burst Switching Network Design," *IEEE Commun. Lett.*, vol. 6, no. 6, pp. 268-270, June 2002.

[13] M. Yoo and C. Qiao, "Just-Enough-Time (JET): A High Speed Protocol for Bursty Traffic in Optical Networks," in *Proc. IEEE/LEOS Conf. on Technologies for a Global Information Infrastructure*, Aug. 1997, pp. 26-27.

[14] M. Yoo, C. Qiao, and S. Dixit, "Optical Burst Switching for Service Differentiation in the Next-Generation Optical Internet," *IEEE. Commun. Mag.*, vol. 39, no. 2, pp. 98-104, Feb. 2001.

[15] R. W. Wolff, *Stochastic Modeling and the Theory of Queues*. New Jersey: Prentice Hall, 1989.